



## RESEARCH ARTICLE SUMMARY

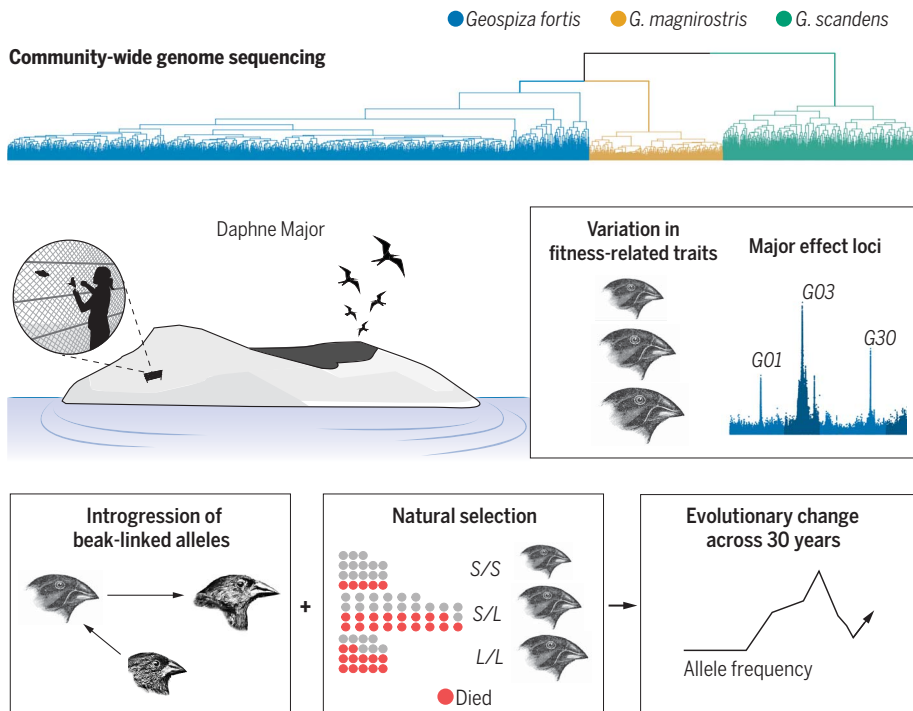
## ADAPTATION

# Community-wide genome sequencing reveals 30 years of Darwin's finch evolution

Erik D. Enbody\*, Ashley T. Sendell-Price, C. Grace Sprehn, Carl-Johan Rubin, Peter M. Visscher, B. Rosemary Grant, Peter R. Grant, Leif Andersson\*

**INTRODUCTION:** Adaptive radiations are groups of organisms that have diverged ecologically from a common ancestor relatively rapidly. They have yielded important insights into the ecology, behavior, and genetics of speciation through inferences of the evolutionary processes that most likely gave rise to observed patterns of divergence. In a few cases, experiments have substantiated these inferences by testing hypotheses of causal mechanisms. Our understanding of evolutionary radiations has been transformed in the past decade by discoveries of the genomic variation underlying phenotypic divergence. The dynamic genomic variation responsible for rapid evolutionary change in contemporary populations in nature, and its connection with evolution in the past, is not well known.

**RATIONALE:** We set out to establish the link between contemporary and past evolution in a well-studied system, Darwin's finches in the Galápagos archipelago. Eighteen species have evolved from a common ancestor in the last million years. They diverged in beak morphology and body size, and to a small extent, in plumage. Two evolutionary processes, natural selection and introgressive hybridization, influenced the outcomes of phenotypic evolution in this adaptive radiation. We followed the fates of individually marked and measured birds of four *Geospiza* species on Daphne Major Island for 40 years to investigate contemporary evolution. We combined observations on fitness with whole-genome sequencing to reveal and interpret the genetic architecture of evolutionary change.



**Evolutionary change revealed by community sequencing.** Population monitoring over 30 years followed by genome-wide sequencing of ~4000 individuals of four Darwin's finch species (the fourth, *G. fuliginosa*, is not visible in the tree) on Daphne Major, Galápagos Islands. Genome-wide association analysis identified major-effect loci on fitness-related traits, revealing alleles transferred among species by introgression and subject to natural selection. S, small beak-size allele L, large beak-size allele.

**RESULTS:** We used whole-genome resequencing data to track evolutionary change in Darwin's finches of four *Geospiza* species. We identified six loci that together explain as much as 45% of variation in beak size of *G. fortis* (medium ground finch), a highly heritable and key ecological trait. One locus alone is responsible for 25% of variation in beak size and 13% of variation in body size, and is most likely a supergene comprising four genes that contain multiple adaptive mutations with phenotypic consequences for both traits. The haplotypes associated with large and small beak size were established before the divergence of *Geospiza* ground finches and *Camarynychus* tree finches. Abrupt changes in allele frequencies at these loci in *G. fortis* resulted from strong natural selection during an extreme drought and explained a large part of the shift in beak size. Introgression of small-beak alleles from the smaller *G. fuliginosa* influenced the outcome of natural selection by increasing the frequency of small alleles in *G. fortis*. In the cactus-feeding *G. scandens* population, we observed more gradual changes in allele frequencies over the study period resulting from introgression.

**CONCLUSION:** We show that a few loci of large effect have had a major impact on the trajectory of Darwin's finch populations on the small island of Daphne Major. They affect fitness through their association with survival in relation to competition for food, particularly during extreme climatic events, and have been passed between species through hybridization. A reasonable explanation for the presence of large-effect alleles in Darwin's finches is that these have evolved over time by the accumulation of multiple causal mutations as a response to diversifying selection. They contribute both to phenotypic differences between species and to phenotypic diversity within *G. fortis*. This genetic architecture differs from the one documented for many polygenic traits in other species lacking large-effect loci, such as beak morphology in some other birds and human stature, which is likely due to differences among species in selection regimes and the impact of gene exchange. These genetic changes at the population level reveal the dynamics of evolutionary change in this iconic adaptive radiation. ■

The list of author affiliations is available in the full article online.  
\*Corresponding author. Email: erik.enbody@gmail.com (E.D.E.); leif.andersson@imbim.uu.se (L.A.)  
Cite this article as E. D. Enbody et al., *Science* 381, eadf6218 (2023). DOI: 10.1126/science.adf6218

**S READ THE FULL ARTICLE AT**  
<https://doi.org/10.1126/science.adf6218>

## RESEARCH ARTICLE

## ADAPTATION

# Community-wide genome sequencing reveals 30 years of Darwin's finch evolution

Erik D. Enbody<sup>1\*</sup>†, Ashley T. Sendell-Price<sup>1</sup>, C. Grace Sprehn<sup>1‡</sup>, Carl-Johan Rubin<sup>1</sup>, Peter M. Visscher<sup>2</sup>, B. Rosemary Grant<sup>3</sup>, Peter R. Grant<sup>3</sup>, Leif Andersson<sup>1,4\*</sup>

A fundamental goal in evolutionary biology is to understand the genetic architecture of adaptive traits. Using whole-genome data of 3955 of Darwin's finches on the Galápagos Island of Daphne Major, we identified six loci of large effect that explain 45% of the variation in the highly heritable beak size of *Geospiza fortis*, a key ecological trait. The major locus is a supergene comprising four genes. Abrupt changes in allele frequencies at the loci accompanied a strong change in beak size caused by natural selection during a drought. A gradual change in *Geospiza scandens* occurred across 30 years as a result of introgressive hybridization with *G. fortis*. This study shows how a few loci with large effect on a fitness-related trait contribute to the genetic potential for rapid adaptive radiation.

The fossil record shows that most long-term evolution is a slow and gradual process (1, 2). By contrast, some extant groups of organisms have diversified from a common ancestor relatively recently into many ecologically differentiated species. These adaptive radiations are the product of especially favorable intrinsic (genetic) potential and extrinsic (environmental) opportunity (3–5). An example of the latter is entry into a new environment relatively free from competitors and predators, such as in the colonization of lakes (6) and islands (3, 7). Less is known about genetic potential, but recent studies have highlighted the relative contribution of genetic architecture, gene flow, and ancestral variation to adaptive radiation (5, 8–10). Theoretical work (11) predicts that diversification can be rapid when few genetic loci of large effect influence adaptive phenotypes and when adaptive introgression is possible. For differences among individuals in a population to propagate to differences among species, these large-effect loci must contribute to individual variation in fitness during incipient speciation. Yet surprisingly little is known of the effect sizes of loci that influence the fitness of individuals in wild populations (12), and how much allele frequencies vary over time because of natural selection (13). Thus,

large-effect loci may play a prominent role in evolutionary change, but the circumstances under which this happens are not clear (14).

Darwin's finches in the Galápagos archipelago are especially suitable for clarifying these issues. The 18 species of this classical adaptive radiation (15, 16) differ principally in beak size, beak shape, and body size, and also to a lesser extent in plumage color and pattern. Beak and body traits of three species in the genus *Geospiza* are highly heritable (16–19). Differences between species reflect dietary specializations (15, 20). Variation in beak- and body-size traits is associated with fitness (survival) in dry seasons of food scarcity, especially during droughts (21), whereas reproductive fitness varies independently of morphological traits (22). Only a small fraction of the genome is strongly differentiated among species of the *Geospiza* ground finches (16, 18, 19, 23), which suggests the possibility that large-effect loci affect fitness (17). These speciation genomics approaches, referred to as reverse genetics (24), need to be combined with forward genetics, that is the direct study of the genetic variation underlying fitness-related traits (25). In this study, we combine these prior insights on variation in beak morphology and body size with a forward genetics approach, motivated by the need to integrate these two levels of analysis (24, 26). To accomplish this, we documented the underlying genetic architecture of morphological traits, the magnitude of the effects of individual loci, and the contribution of natural selection and introgressive hybridization to the fluctuations in allele frequencies at these loci.

We collected data from 3955 individuals from a community of four species of *Geospiza* ground finches (*G. fortis*, *G. fuliginosa*, *G. magnirostris*, and *G. scandens*) in their shared environment of Daphne Major Island each year for more

than 30 years and measured their phenotypic evolution, genomic composition, and fitness variation. Finches were marked with distinct combinations of colored leg bands to allow direct determination of individual fitness (survival). We identified, quantified, and documented the importance of six large-effect loci and showed how allelic variation has changed under contrasting influences of natural selection and introgressive hybridization. One of the loci comprising four genes in strong linkage disequilibrium (LD) acts as a supergene. Extrapolating from these findings, we suggest that a few loci of large effect contributed disproportionately to the rapid diversification of species in this classical example of adaptive radiation. These findings demonstrate the potential to leverage long-term genomic monitoring to understand short- and long-term processes that shape natural populations.

## Results

### Whole-genome community analysis over multiple generations

Blood samples were collected annually from the four species of finches on Daphne in the years 1988 to 2012 (from individuals hatched as early as 1983). We performed low-pass, whole-genome sequencing for all individuals captured. In total, we sequenced 3955 individuals to a mean depth of 2.2×, comprising 1909 *G. fortis*, 852 *G. scandens*, 582 *G. magnirostris*, 55 *G. fuliginosa*, and 555 individuals of hybrid origin (table S1). For 2543 individuals sampled as adults, we measured three beak dimensions (length, depth, and width), body weight, and recorded sex when known. To identify single-nucleotide polymorphisms (SNPs), we used an iterative imputation pipeline with a reference panel of 433 Darwin's finches sequenced to higher coverage (15 ± 8×), a de novo pedigree-based recombination map (fig. S1), and the software GLIMPSE (27), which imputes genotypes based on genotype likelihoods ( $n_{\text{SNPs}} = 5,163,840$ ). We found high concordance for imputed variants that have reference panel allele frequencies >0.5% (fig. S2) and, at the genome-wide level, high correlation between the first two components of a principal component analysis (PCA) using imputed genotypes versus genotype likelihoods (fig. S3).

### Admixture and immigration are important components of population history

Genome-wide divergence is low among the four *Geospiza* species on Daphne ( $F_{\text{ST}} = 0.03$  to 0.17). To track the ancestry of every individual on the island, we estimated genomic ancestry (i.e., the contribution of historical population structure to an individual's genetic constitution) using a set of ancestry-informative, putatively neutral, and unlinked markers (28). Daphne finches show extensive

<sup>1</sup>Department of Medical Biochemistry and Microbiology, Uppsala University, Box 582, 751 23 Uppsala, Sweden.

<sup>2</sup>Institute for Molecular Bioscience, The University of Queensland, 306 Carmody Rd., St. Lucia QLD 4072, Australia. <sup>3</sup>Department of Ecology and Evolutionary Biology, Princeton University, 106A Guyot Hall, Princeton, NJ 08544, USA. <sup>4</sup>Department of Veterinary Integrative Biosciences, Texas A&M University, 402 Raymond Stotzer Pkwy Building 2, College Station, TX 77843, USA.

\*Corresponding author. Email: erik.enbody@gmail.com (E.D.E.); leif.andersson@imbim.uu.se (L.A.)

†Present address: Department of Biomolecular Engineering, University of California, Santa Cruz, CA 95064, USA.

‡Present address: DOE Joint Genome Institute, Lawrence Berkeley National Laboratory, Berkeley, CA 94720, USA.

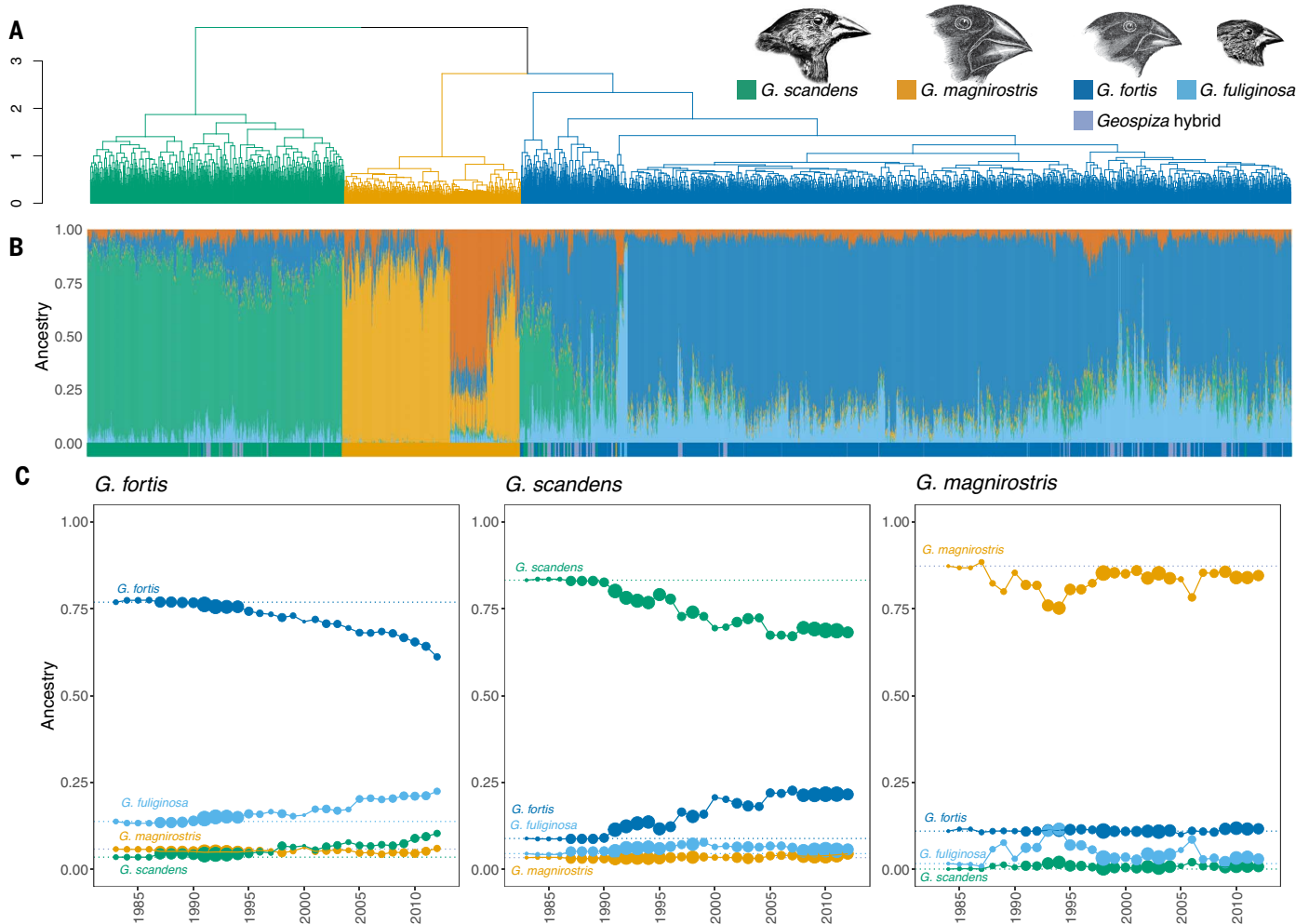


**Fig. 1. Admixture history of four species of finches on Daphne Major.**

(A) Clustering derived from the relatedness matrix produced by using genome-wide SNPs in the software GEMMA. (B) Ancestry estimates ( $K = 5$ ) for each of 3955 individuals on Daphne based on ancestry-informative SNPs. Filled column colors designate the proportion of ancestry from each of the five ancestral populations, representing the four species, plus a second *G. magnirostris* population

in dark orange. Below, filled horizontal bars designate the field identification, including a hybrid classification (purple). (C) Annual trends in ancestry per species grouping from  $K = 4$ . Each panel refers to the field identification labeled above. Ancestry estimates are the mean value per cohort each year starting in 1983 and ending in 2012. Illustrations of the four species are adapted from P.R.G. and Darwin (83).

signatures of admixture (Fig. 1), which is consistent with previous genomic and pedigree-based observations (29–32). Reflecting the accumulated effect of introgression, set in motion by ecological changes in the 1980s by two unusually intense El Niño events (33), finch species were more genetically differentiated at the beginning than at the end of the study period; self-ancestry (e.g., *G. fortis* in *G. fortis*) declined 20% in *G. fortis*, 17% in *G. scandens*, and 0.2% in *G. magnirostris* (Fig. 1C). These are likely the lower bounds of ancestry owing to high allele sharing across the radiation (16). The largest introgression of genomic material in *G. scandens* is from *G. fortis*, which increased by 12%. By contrast, the largest contribution to the *G. fortis* population originates from *G. fuliginosa*, whose contribution to *G. fortis* increased by 14%. These directions of introgression are consistent with

pedigree information (32). By contrast, interspecific ancestry in the noninterbreeding species *G. magnirostris* remained close to zero throughout (Fig. 1C).

Changes in ancestry are strongly correlated with phenotypic shifts. Variation in beak morphology among the four Daphne finch species can be decomposed into two principal components that explain 99.7% of morphological variation, with principal component 1 (PC1) loading on beak size (referred to as beak size hereafter) and PC2 on beak shape (referred to as beak shape hereafter) (Fig. 2A). In *G. fortis*, change in beak shape is significantly correlated with the introgression of genomic material from *G. scandens* (ancestry-phenotype correlation,  $R^2 = 0.23$ ; fig. S4A) and change in beak size, with introgression from *G. fuliginosa* ( $R^2 = 0.12$ ; fig. S4B). In *G. scandens*, introgression from *G. fortis* is correlated with beak shape ( $R^2 =$

0.3; fig. S4C), and *G. fortis* and *G. fuliginosa* both contribute to a change in beak size, but to a small extent ( $R^2 = 0.04$  and  $R^2 = 0.01$ ; fig. S4D). Changes in shared ancestry between *G. fuliginosa* and *G. scandens* are noteworthy because these species have not been recorded hybridizing on Daphne in 40 years of intense study of the breeding populations (32). We tracked a haplotype that is associated with *G. fuliginosa* ancestry and found that this haplotype has increased in *G. scandens* over time (supplementary note 1 and fig. S5), which supports field observations and microsatellite analysis that *G. fortis* is a conduit species for introgression from *G. fuliginosa* to *G. scandens* (32).

The estimated number of ancestral populations on Daphne is a good fit to  $K = 4$  or  $K = 5$ , i.e., one more than the expected number of species (fig. S6). At  $K = 5$ , the fifth population reflects

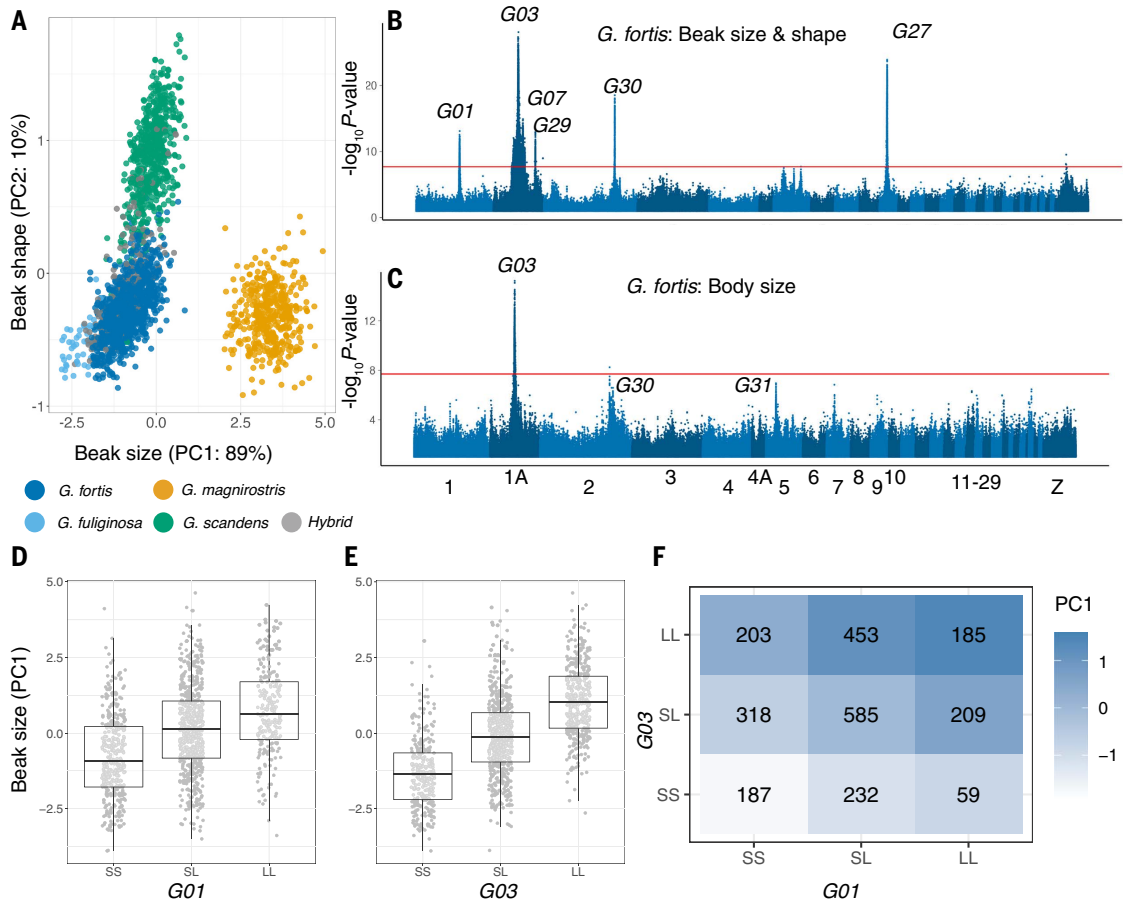


**Fig. 2. Genome-wide association analysis of morphological variation in beak and body size in *G. fortis*.** (A) Morphological PCA for beak width, length, and depth, colored by species with hybrids in gray. PC1 explains 89% of variation and PC2 explains 10%. (B) Multivariate GWAS for beak PC1 and PC2, including body weight and sex as covariates. The cutoff for genome-wide significance at  $-\log_{10}(P \text{ value}) = 7.7$  is indicated. Locus names match and extend those previously reported (23). (C) GWAS for body weight with sex as a covariate.

G30 and G31 are highlighted despite falling short of the significance threshold. (D and E) Relationships between G01 and G03 genotypes and beak size. Genotypes are coded according to carrying the phenotypically small (S) or large (L) allele. (F) Heatmap that demonstrates phenotypic effects of all genotype combinations at G01 and G03, with sample sizes written within quadrants; positive or negative values mean that a beak size is larger or smaller than the average, respectively.

heterogeneity in the Daphne *G. magnirostris* breeding population. A single pair of individuals initiated the Daphne *G. magnirostris* population, which was later augmented by immigrants (34). Our ancestry analysis identified two sources of immigrants to Daphne: one from a nearby island (Santa Cruz, Marchena, or Isabela), and a second that was ~5% larger in size from an as-yet-unknown island of origin (fig. S7 and supplementary note 2). These results highlight the dual contributions of hybridization and immigration to genetic and phenotypic diversity on Daphne.

#### High SNP heritability of beak morphology and body size

Heritability of beak traits in *Geospiza* ground finches is high (35). To determine the power for studying the genetic architecture of morphological traits, we independently calculated SNP heritability ( $h^2_{\text{SNP}}$ ) of beak morphology and body size.  $h^2_{\text{SNP}}$  is an estimate of the pro-

portion of variance in phenotypic traits explained by our imputed SNP dataset. This can be biased by local variation in LD, so to account for this bias when estimating  $h^2_{\text{SNP}}$ , we used an analysis of LD and minor allele frequency (MAF)-stratified residual maximum likelihood (GREML-LDMS) as implemented in the software package GCTA (36). Here, we analyzed three phenotypic traits, beak size, beak shape, and body size, by using individuals with complete phenotypic data ( $n = 2545$ ). We ran all association analyses separately on three genetic clusters (Fig. 1A) that were representative of *G. fortis* ( $n = 1508$ ), *G. scandens* ( $n = 552$ ), and *G. magnirostris* ( $n = 430$ ). We did not include *G. fuliginosa* samples in this analysis because of low power for genotype-phenotype analysis ( $n = 55$ ).

We estimated a total beak size  $h^2_{\text{SNP}}$  in *G. fortis* of 0.95 (SE = 0.02). A large proportion of this estimate is captured by common (MAF > 0.05) and high-LD variants ( $h^2_{\text{SNP}} = 0.77$ , SE = 0.04) (fig. S8). Heritability of beak shape ( $h^2_{\text{SNP}} =$

0.78, SE = 0.03) (fig. S8) and body size ( $h^2_{\text{SNP}} = 0.67$ , SE = 0.04) (fig. S8) are also high (33, 35). The high SNP-based estimates match pedigree  $h^2$  (33, 35) and confirm that beak traits and body size are highly heritable in Darwin's finches. High estimates provide an opportunity for genotype-phenotype analysis.

#### GWAS identifies large-effect loci underlying ecological traits

To identify loci underlying phenotypic variation, we performed a genome-wide association study (GWAS) using the software GEMMA (37). Because beak and body size (weight) are strongly correlated (*G. fortis*,  $r = 0.74$ ,  $P < 0.001$ ), we included body weight as a covariate in a multivariate GWAS of beak size (PC1) and shape (PC2) as the response variables. For beak size and shape in *G. fortis*, we identified six independent loci surpassing a significance threshold of  $-\log_{10}(P) > 7.7$  set by permutation (Fig. 2B; Fig. 3, A to D; fig. S9, and supplementary note 3).

A large region of significant association spanning 4.3 Mb on chromosome 1A contains the previously identified *G03* locus that encompasses *HMG2* and three other genes (Fig. 3B) (17). An exploratory analysis indicated that the

majority of this large region is behaving as a single locus in the *G. fortis* population on Daphne (fig. S10). We identified the same six loci using a leave-one-out chromosome approach (fig. S11 and supplementary Note 4).

We analyzed body weight using the relatedness matrix and sex as covariates. In *G. fortis*, we identified a large-effect locus *G03* on chromosome 1A and two additional loci, *G30* and *G31*, that approached genome-wide significance

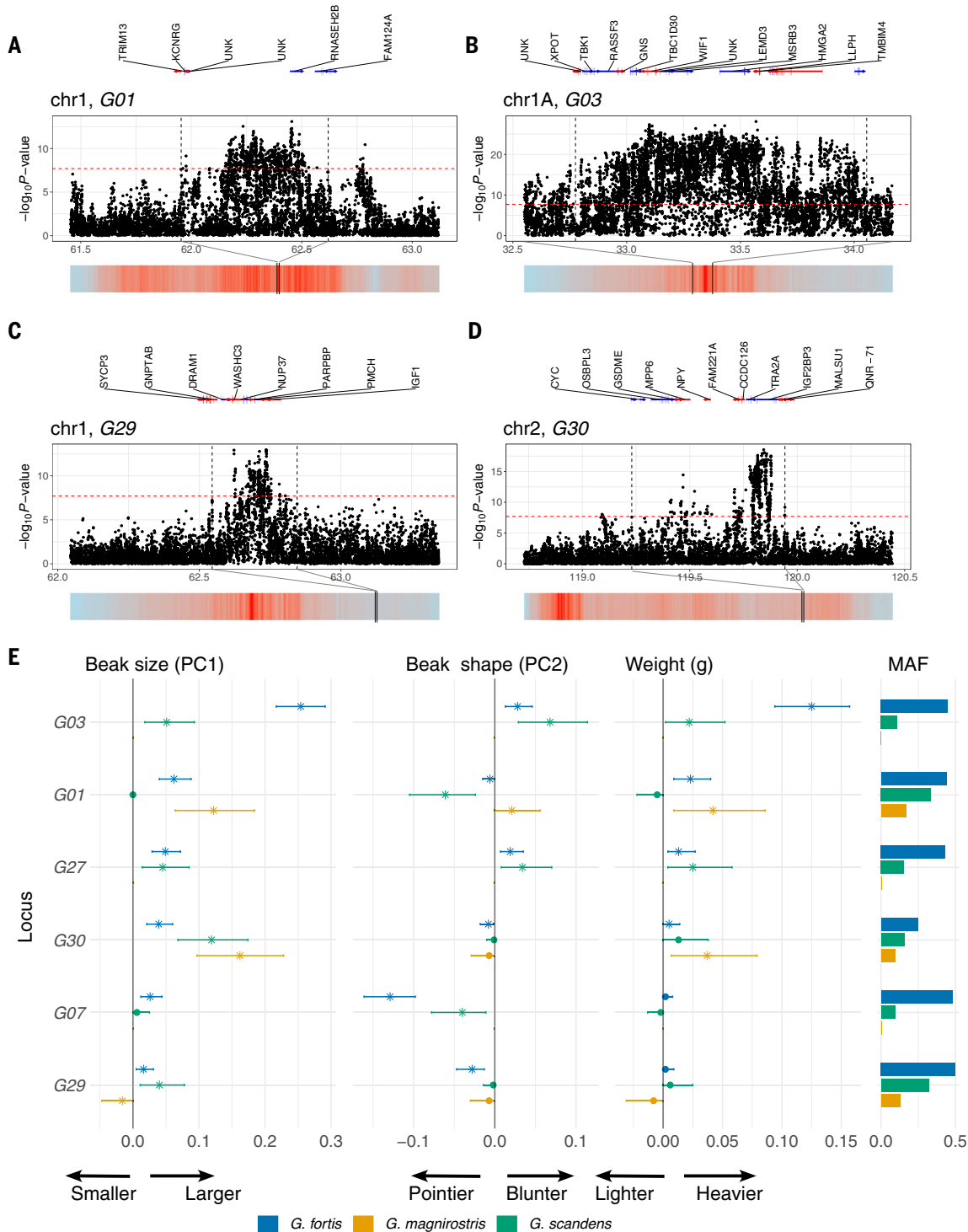


**Fig. 3. Details of association peaks and estimated additive effects.** (A to D) Zoom-ins of regions of associations for loci *G01*, *G03*, *G29*, and *G30* in *G. fortis*. Below each, a heatmap of a sliding window of LD of all SNPs in 200-kb windows (blue, low; red, high). Chr, chromosome. (E) Additive effect-size predictions for each of the six loci shown in Fig. 2B. Colors indicate the three species, error bars denote 95% confidence levels, and an asterisk designates statistical significance [ $P < 0.05$ ; (28)]. (Right) The MAF within species for each locus. *G. magnirostris* is fixed for the large allele at *G03*, *G07*, and *G27*.

(Fig. 2C). Thus, *G03* has a large effect on body weight, and separately on beak size, independent of body weight. Four of the six loci that control beak size in *G. fortis* also reach statistical significance in *G. scandens*, but only one (*G01*) does so in *G. magnirostris* (figs S12 and S13). Weaker associations in these species may reflect the smaller sample sizes (by a factor of 3 or more) and less within-group variation at these loci. For example, *G. magnirostris* is nearly fixed for one allele at both *G03* and *G30* (and therefore, these loci are not detected in these species) (fig. S13). A notable feature of *G. scandens* is an association of a single large region (34 Mb) on chromosome 5 with beak phenotype (fig. S13). This region harbors large divergent haplotypes (fig. S14) and overlaps a region known to be resistant to introgression from *G. fortis* to *G. scandens* (29).

Two loci (*G29* and *G30*) have not been previously associated with individual variation in Darwin's finches, and each contains insulin-like growth factor-related genes (*IGF1* and *IGF2BP3*, Fig. 3, C and D, respectively). These genes are part of a well-characterized network involved in growth, metabolism, and aging (38–41). IGFs are also associated with beak size in *Pyrenestes oestrinus* (42) and the evolution of life-history variation across amniotes (43). A third IGF-related gene, *IGF2*, falls just short of genome-wide significance in the body-size GWAS in *G. fortis* (*G31*). Together with the previously reported *G26* (*IGFBP2*) locus (23), the identification of four *IGF* loci associated with Darwin's finch beak morphology supports the hypothesis that gene networks involved in this pathway coevolve (43).

### Effect sizes

To estimate effect sizes, we identified haplotypes associated with each GWAS signal (region size, 0.2 to 4.3 Mb). When combined, the six loci account for 45% of the variation in beak size and 22% of the variation in beak shape in *G. fortis* (Fig. 3E). These values decline to 29 and 22%, respectively, after controlling for the correlated effects of body size by using residuals of a model that includes body weight and sex as covariates. Similarly, in *G. scandens*, these six loci account for 26% of beak size (residuals = 28%) and 21% of beak shape (residuals = 18%). Only three loci (*G01*, *G29*, *G30*) segregate in *G. magnirostris*, but cumulatively they explain 30% (residuals = 23%) of variation in beak size (Fig. 3E). All loci contribute additively to beak size variation in *G. fortis* (Fig. 2, D to F, and fig. S16). When we fitted these six loci as covariates in a GREML analysis of *G. fortis*, we found that they explain 59% of total  $h^2_{\text{SNP}}$  in beak size, 17% of the variation in weight, but only 3% of beak shape (fig. S17). Thus, a small number of loci explain a large portion of the heritable beak size variation in *G. fortis*. Effect-size estimations were

largely robust to filtering based on genomic ancestry estimates, which suggests that their magnitude is not inflated by background ancestry (fig. S18).

The single largest contributor to beak size is *G03*, which alone accounts for 25% of beak size variation in *G. fortis* (Fig. 3E and table S2), half of the total explained variation (45%). This was reduced to 12% after we controlled for the correlated effect of body size (fig. S15 and table S2). The remaining five loci explain between 2% (*G29*) and 6% (*G01*) of beak size variation in *G. fortis*. Approximately 14% of beak shape variation in this species is explained by another locus (*G07*) after the effects of body size are controlled. Across species, we detected heterogeneity at four loci associated with beak morphology in *G. scandens* (28) (supplementary Note 5). These loci imply that species-specific polymorphisms occur even on shared haplotypes.

Previously, we identified 28 loci with large allele-frequency differences among *Geospiza* species (23). We reduced them to 14 distinct loci after LD pruning (fig. S19) to eliminate those in strong LD within the *G. fortis* population on Daphne. Four reached genome-wide significance in the present study (*G01*, *G03*, *G07*, and *G27*). Six out of the 10 remaining loci either had small effects on beak size (four loci explained <1% of variation) (fig. S20) or explained 1 to 2% of variation in beak shape (two loci) (fig. S20). In all six cases, the allele associated with a large beak in the *G. fortis* population on Daphne is the most common in the largest species, *G. magnirostris*, rare in the smallest species, *G. fuliginosa*, and at intermediate frequency in *G. fortis* (fig. S20). Together, these results indicate that species differences in allele frequencies associated with beak and body size are largely recapitulated in individual variation in *G. fortis*.

### Candidate mutations

Identifying candidate causal genes and mutations can link quantitative trait loci (QTL) to the underlying molecular mechanisms. Therefore, we compiled a list of all SNPs and small insertions and deletions (indels) at the six loci affecting beak size in *Geospiza* with change in allele frequencies ( $\Delta\text{AF}$ )  $\geq 0.9$  between large and small haplotypes. Of these 3556 SNPs, 12 were missense, 11 were synonymous, and 102 sequence variants occurred at noncoding sites with high sequence conservation scores (77-way Vertebrate PhyloP  $\geq 2$ ) (table S3). This revealed two general observations. First, only three of the six beak loci harbor missense mutations with  $\Delta\text{AF} \geq 0.9$ , which, together with the abundance of conserved noncoding changes, suggests that regulatory mutations are important for the observed QTL effects. Second, 7 out of 12 (58%) missense mutations were located in locus *G07*. Two are in the transcription

factor gene *ALXI*, which has a well-established role in craniofacial development in vertebrates (44) and is expressed during beak development in Darwin's finches and in the zebra finch (23). Four out of the five additional missense mutations in *G07* occur in *LRR1Q1*, a gene previously implicated in *Parus major* beak variation (45). The function of the *LRR1Q1* protein is poorly characterized, but it includes a calmodulin-binding domain (46) that may interact with the calmodulin pathway, a gene network previously implicated during development in Darwin's finches (47). The presence of seven missense mutations close to fixation among the haplotypes at the *G07* locus supports the prediction that this locus harbors multiple causal mutations and may act as a supergene (48).

### The *G03* locus is a supergene

The large region overlapping *G03* is the most important locus affecting body and beak size in the *G. fortis* population on Daphne Major (Fig. 2, B and C). *G03* was previously defined as a 525-kb region based on a comparison among species (17, 23). Within this smaller region, the *Small* (*S*) beak haplotype is close to fixation in *G. fuliginosa*, the *Large* (*L*) haplotype is close to fixation in *G. magnirostris* and *G. scandens*, whereas the two alleles segregate at intermediate frequencies in *G. fortis*. By combining haplotype data from these four species on Daphne, we recovered a 525-kb region with  $\Delta\text{AF}$  approaching 1.0 between the *S* and *L* haplotypes (Fig. 4, top). These haplotypes also segregate in *Camarhynchus* tree finches (23), with  $\Delta\text{AF}$ s approaching 1.0 in each of two distinct regions (Fig. 4, bottom). *G03* haplotypes for the 525-kb region are conserved in the four *Geospiza* and the three *Camarhynchus* species, which suggests that they predate the split between ground and tree finches (Fig. 4). Notably, LD is not homogeneous across the region, as would be expected for an inversion-associated supergene. The shared LD pattern in *Geospiza* and *Camarhynchus* shows (i) near-complete LD within each of the two regions with the highest  $\Delta\text{AF}$ s, one containing *WIF1/LEMD3/MSRB3* and one containing *HMG2*; (ii) near-complete LD between these two regions; and (iii) an area between these two regions with lower  $\Delta\text{AF}$ s among haplotypes and incomplete LD to the two regions (Fig. 4). By contrast, the gray warbler finch (*Certhidea fusca*, sister to all other finch species) shows no strong LD in the corresponding region (fig. S21). These findings are inconsistent with a single mutation with pleiotropic effects on body and beak size in *Geospiza* and *Camarhynchus*. Instead, we propose that *G03* is a supergene involving four genes and causal mutations with epistatic interactions.

The identification of two core regions of association provides a potential explanation for

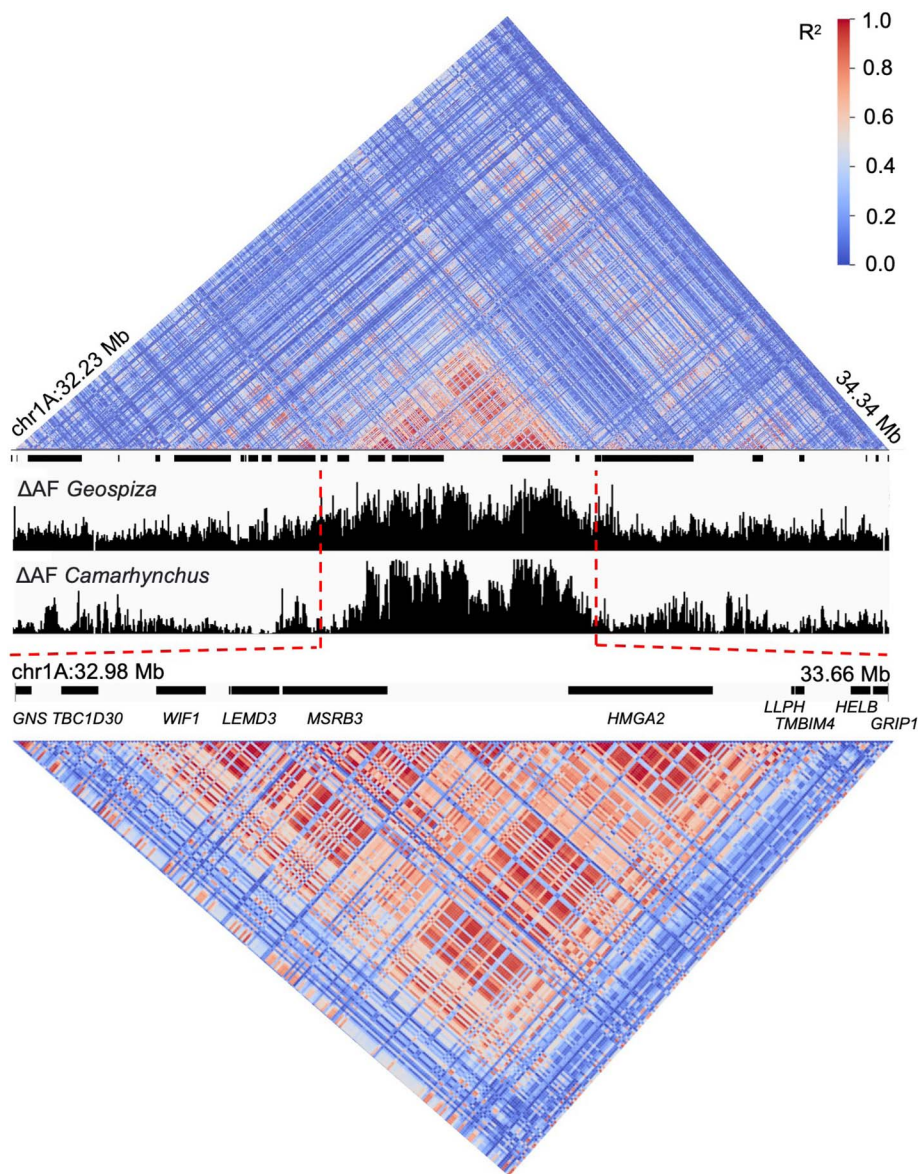


**Fig. 4.** LD patterns from combined *Geospiza* and *Camarhynchus* individuals and  $\Delta AF$ . (Top) LD for a 2.1-Mb region of locus *G03*, with gene models indicated as black bars beneath. (Middle)  $\Delta AF$  between *S* and *L* alleles in *Geospiza* or *Camarhynchus*. (Bottom) An enlarged region of high LD; black bars represent gene regions.

the pleiotropic effect of *G03* on both beak and body size. One region contains *HMGA2*, a transcription-facilitating factor gene. *HMGA2* is one of the top four loci associated with variation in human stature and explains about 0.3% of genetic variance (49). It has major effects on body size in other vertebrates (50–53), and null alleles cause dwarf phenotypes in mice (54), rabbits (55), and pigs (56). We hypothesize that noncoding polymorphisms that affect *HMGA2* expression cause a change in both body and beak size, whereas the additional, independent effect on beak size (Fig. 2B) may be controlled by mutation(s) in one or more of the other genes at the *G03* locus. Among these three genes, *LEMD3* is an interesting candidate (Fig. 4), because loss-of-function

mutations cause bone density disorders in humans. Further, the *LEMD3* protein interacts with bone morphogenic protein (BMP) signaling (57). Differential expression of *BMP4* is associated with variation in beak morphology in Darwin's finches (58), although the gene is not associated with a significant QTL effect on beak phenotypes.

#### Natural selection and introgressive hybridization change allele frequencies at major effect loci

The average size of *G. fortis* and *G. scandens* beak dimensions oscillated in response to changing ecological conditions over the 30 years of monitoring (Fig. 5A) (33, 59). Changes in allele frequency at the six large-effect loci identified in our GWAS changed concordantly with mor-

phology, generally exceeding annual shifts in allele frequency at random loci (Fig. 5, B and C, and fig. S22). The strongest shift occurred in *G. fortis* during 2.5 years of drought from late 2003 to early 2005 (60). The beaks of *G. fortis* became smaller on average because of differential mortality resulting from competition with the much larger *G. magnirostris*. The frequency of the *G03 S* allele (Fig. 5A) increased sharply from 0.50 in 2004 to 0.63 in 2005 (17). In a generalized linear-mixed model, *G03* alone predicts survival with a selection coefficient of 0.49 (Fisher's exact test,  $P < 0.05$ ). Three other loci show a very similar change with an increase of the allele associated with small beak size (and two others trend in this direction). Indeed, three loci (*G01*, *G03*, and *G29*) in combination predict survival from 2004 to 2005 better than *G03* alone in a repeated leave-one-out analysis [Akaike information criterion (AIC);  $AIC_{combined} = 89.4$  versus  $AIC_{G03} = 97.6$ ] ( $z = 3.1$ ,  $P < 0.01$ ) (Fig. 5D). Shifts in allele frequencies at these three loci can account for 51% of the phenotypic shift in beak size due to natural selection.

Changes in ancestry (Fig. 1C) affected allele frequencies at these six loci. Allele frequency changes at the six loci (2 to 30%) are greater in *G. fortis* than in *G. scandens* (1 to 10%) (Fig. 5A). The phenotypic change toward a blunter beak in *G. scandens* is the outcome of incremental gene flow from *G. fortis* beginning in the 1990s (Fig. 1C) (29, 59). A spike in allele-frequency change at the turn of the century (Fig. 5C) is likely due to this introgression in the El Niño year of 1998: The frequency of hybridization increased in the next two dry years with no breeding when many finches died from starvation, and then decreased in the following year (Fig. 1) (33). At the locus with the largest phenotypic effect on beak shape (*G07/ALXI*), *G. scandens* carrying a *Blunt* allele were more likely to have *G. fortis* ancestry than those carrying a *Pointed* allele (Generalized linear model, GLM:  $F = 1.1$ ,  $P < 0.0001$ ; fig. S23A and supplementary note 1). Similarly, *G. fortis* carrying the *S* allele at *G03*, the locus of greatest phenotypic effect on beak size, were more likely to have *G. fuliginosa* ancestry (GLM:  $F = -1.1$ ,  $P < 0.0001$ ; fig. S23B) and *G. fuliginosa*-associated SNPs (fig. S23, C and D). *G. fortis* and *G. scandens* converged in allele frequency at *G07* but diverged at *G03* (Fig. 5F). Divergence is a consequence of hybridization between *G. fortis* and *G. fuliginosa* and strong selection in the 2004–2005 period, resulting in a higher frequency of the *S* allele at *G03* in *G. fortis* (Fig. 5, E and F).

#### Conclusions

We describe the genetic architecture underlying morphological traits and temporal variation in fitness in a natural community of Darwin's finches on the undisturbed island of Daphne

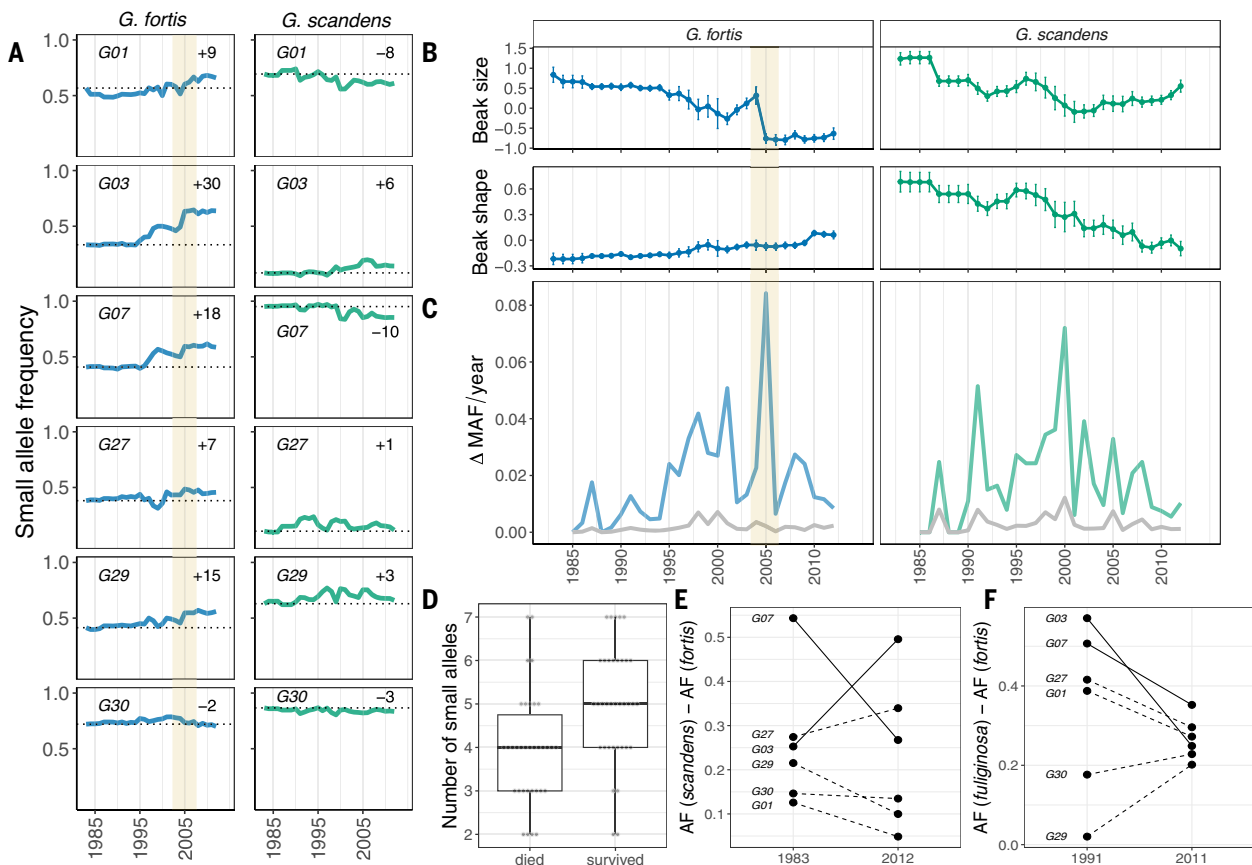


**Fig. 5. Evolutionary change over 30 years on Daphne Major.** (A) Annual allele frequency trajectories at each of the six loci in *G. fortis* and *G. scandens*. (B) Annual phenotypic means for *G. fortis* and *G. scandens* between 1983 and 2012. (C) The absolute average change in allele frequency [ $\Delta AF = \text{abs}(AF_{\text{year}n} - AF_{\text{year}n-1})$ ] across all six loci shown in Fig. 2. The colored line indicates the average of all six loci and the gray line indicates 100 randomly selected loci across the genomes with starting allele frequencies that match the six loci. The yellow bar highlights in (A) and (B) denote the 2004 to 2005 drought event.

(D) The total number of small alleles at *G01*, *G03*, and *G29* differs between individuals that survived or died in the 2004/2005 drought event. (E)  $\Delta AF$  between *G. scandens* and *G. fortis* early compared with late in the study period. *G07* and *G03* are highlighted with solid lines, with *G07* becoming more similar among the two species and *G03*, more different. (F) Same as (E), but comparing *G. fuliginosa* and *G. fortis* early and late in the study period, where both *G07* and *G03* have converged in frequency. Additional discussion of *G07* can be found in supplementary note 1.

Major, Galápagos. The study encompassed lowpass, whole-genome sequencing of nearly 4000 birds from more than 30 years and 5 to 10 generations. We report that six loci are collectively responsible for as much as 45% of the genetic variance in beak size in *G. fortis*. One locus (*G03*) explains 25% of the variance, partly through correlated effects of body size and partly (12%) through direct effects independent of body size. Allele frequencies at the six loci in *G. fortis* and *G. scandens* changed as a result of episodic natural selection and recurring introgressive hybridization. Because allele frequencies differ among species (23), these multi-decade observations of allele dynamics provide the basis for a genetic understanding of speciation over a much longer period.

The field-standard geometric model is dominated by many loci of small effect (61, 62). Darwin's finches are clearly toward one extreme of variation in effect-size distributions. Empirical studies with a comparable experi-

mental design (i.e., sample size and methodology) and that use quantitative traits with high heritability are not yet available for other birds. Therefore, for comparison, we turn to humans because stature has a heritability as high as that of beak traits in Darwin's finches ( $h^2 \sim 0.80$ ), and effect sizes are estimated from millions of individuals (49). However, the selection pressures affecting human stature differ from those affecting beak size, which influences the distribution of effect sizes (63). Nevertheless, human stature is the most studied quantitative trait in any animal (49) and is useful to place our results in context. For example, a GWAS on humans from the UK Biobank that used a sample size identical to the one used here for *G. fortis* ( $n = 1508$ ) has only 20% power to detect a single QTL that reaches genome-wide significance (fig. S24) because the variance explained by individual loci is small. The top six loci from a recent GWAS study (49), based on 5.4 million individuals,

only explain about 1% of the variance in contrast to the 45 and 22% of the explained variance for beak size and beak shape, respectively, in Darwin's finches. *HMG2* provides a stark contrast. The *G03* locus that includes *HMG2* explains 25 and 13% of variation in beak size and body size, respectively, whereas *HMG2*, one of the top six loci in humans, explains only 0.3% of variation in stature (49). Human stature is likely under stabilizing selection, meaning that large-effect alleles are detrimental (64, 65), occur at low frequencies, and contribute little to trait variance. Conditions that vary over time may instead lead to balancing selection and the maintenance of variation, rather than the fixation of beneficial alleles, because of fluctuations in the fitness of alleles at individual loci. This is the case in the Galápagos, where oscillating environmental conditions that lack predictability have unpredictable evolutionary outcomes (59). We found substantial shifts in allele frequencies at these



loci under periods of environmental stress and intense interspecies competition in *G. fortis*, which has an intermediate phenotype and genotype (Fig. 5). The loci may have particularly large effects because they have been subject to divergent selection during the evolution of Darwin's finches. Strong selection on beak size has driven alternative *G03* alleles close to fixation in the large (*G. magnirostris*) and small (*G. fuliginosa*) species, but their large phenotypic effects are observed in *G. fortis*, where they are subject to oscillating directional selection. These findings offer a snapshot into the population-level processes that underlie the long-term processes of speciation and adaptive radiation.

A second feature of interest in the genetic architecture of phenotypes, in addition to effect sizes of individual loci, is the physical arrangement and interactions of genes on chromosomes. We identified large genomic regions acting as supergenes, which are clusters of closely linked genes in which haplotypes that control one or more phenotypic traits are inherited as alleles at a single locus owing to suppressed recombination, often due to the presence of inversions (66, 67). The LD pattern for the ~525-kb *G03* haplotypes associated with large and small beak size predates the split between *Geospiza* and *Camarhynchus*, dated 400,000 years ago (16). This implies that *G03* is a supergene composed of multiple sequence variants that show epistatic interaction. It is improbable that such large haplotype blocks can be maintained over ~400,000 years without strong selection and suppressed recombination. There is no indication that the *G03* region involves an inversion, but it occurs in a low recombination region (23), and rare recombinant haplotypes with low fitness may be eliminated by selection. Approximately 7 Mb from the *G03* region is another locus, *G07* (*ALX1*), which was suggested to be a supergene in a previous study (48). The two regions are separated by a recombination hotspot (23). This observation supports the prediction that clusters of adapted loci are formed during local adaptation (67, 68) and have an important role during adaptive radiation (5).

A third important factor is gene flow between closely related populations. Gene exchange modulates the segregation of large-effect alleles in Darwin's finches and in other species (12, 69). Our results support theoretical predictions from simulations that adaptive radiation is likely to involve loci of large effect (11), and that the evolution of the effect size of fitness-related traits is predicted to move toward fewer loci of large effect (and multiple linked sites) when selection for local adaptation takes place with ongoing gene flow (68, 70). This factor likely contributes to differences between our results and a reported polygenic basis for beak variation that lacks large-effect loci in

*Passer domesticus* (71) and *Parus major* (45). Both species are widespread with large effective population sizes that are unaffected by introgressive hybridization.

Adaptive radiations are the product of a favorable genetic potential and environmental opportunity for evolutionary change (3–5). The value of Darwin's finches lies in what they reveal about these features in the early stages of speciation in a young adaptive radiation, when ecological divergence has occurred repeatedly and strongly but without the kind of genetic divergence that impairs fertility and viability (72). Focusing on genetic potential, we have shown that a few identified loci have large effects, individually and in combination, on quantitative, fitness-related, phenotypic traits. Allele frequencies at the loci fluctuate through directional natural selection and introgressive hybridization, thereby revealing the evolutionary dynamics of a classical case of adaptive radiation.

### Materials and methods

Detailed materials and methods can be found in the supplementary materials (28).

### Sample preparation and genotype imputation

Blood samples were collected from Darwin's finches on Daphne Major and other Galápagos islands by P.R.G. using methods described elsewhere (16, 17, 33), and all phenotypic measurements were collected by P.R.G. This included 3955 finches on Daphne Major, and we generated Tn5 transposon-based whole-genome libraries for low-coverage short-read sequencing (73–75). Among these samples are 607 samples of both *G. fortis* and *G. scandens* used in a recent publication (73). We created a reference panel of individuals with high-confidence variant sites for all 18 species of Galápagos finches and two outgroup species. This panel consisted of previously published (16, 17, 23) and new sequencing data generated in this study (supplementary materials). To create our reference panel, we statistically inferred haplotypes using a combination of WhatsHap (76) (v0.18) and SHAPEIT4 (77) (v4.L3). For all low-coverage individuals, we imputed variable sites using GLIMPSE (27) (V1.1), aided by a recombination map generated with 818 *Geospiza* families and *Lep-MAP3* (78).

### Genomic analysis

For the four species on Daphne Major (*G. fortis*, *G. scandens*, *G. fuliginosa*, and *G. magnirostris*), we generated a set of ancestry-informative markers using samples collected from other islands in the archipelago. Using these ancestry-informative markers, we ran ADMIXTURE v1.3.0 (79) on all Daphne samples to estimate ancestry coefficients for every individual. We conducted a GWAS using linear mixed models with the software GEMMA (37) and GCTA (80)

to identify QTLs associated with beak morphology and body size. After identifying loci with strong associations, we identified haplotypes that are associated with each QTL. Analysis of effect sizes and the association between allele frequencies at these loci and ecological and other biotic factors were all conducted by using these haplotype identifications. We searched for variants with putative functional consequences using a combination of variant effect analysis in snpEff (81) and phylogenetic conservation score analysis based on PhyloP.

### REFERENCES AND NOTES

- G. G. Simpson, *Tempo and Mode in Evolution* (Columbia Univ. Press, 1944).
- A. R. Evans *et al.*, The maximum rate of mammal evolution. *Proc. Natl. Acad. Sci. U.S.A.* **109**, 4187–4190 (2012). doi: [10.1073/pnas.1120774109](https://doi.org/10.1073/pnas.1120774109); pmid: [22308461](https://pubmed.ncbi.nlm.nih.gov/22308461/)
- R. G. Gillespie *et al.*, Comparing adaptive radiations across space, time, and taxa. *J. Hered.* **111**, 1–20 (2020). doi: [10.1093/jhered/esz064](https://doi.org/10.1093/jhered/esz064); pmid: [31958131](https://pubmed.ncbi.nlm.nih.gov/31958131/)
- J. I. Meier *et al.*, The coincidence of ecological opportunity with hybridization explains rapid adaptive radiation in Lake Mweru cichlid fishes. *Nat. Commun.* **10**, 5391 (2019). doi: [10.1038/s41467-019-13278-z](https://doi.org/10.1038/s41467-019-13278-z); pmid: [31796733](https://pubmed.ncbi.nlm.nih.gov/31796733/)
- D. A. Marques, J. I. Meier, O. Seehausen, A combinatorial view on speciation and adaptive radiation. *Trends Ecol. Evol.* **34**, 531–544 (2019). doi: [10.1016/j.tree.2019.02.008](https://doi.org/10.1016/j.tree.2019.02.008); pmid: [30885412](https://pubmed.ncbi.nlm.nih.gov/30885412/)
- O. Seehausen, C. E. Wagner, Speciation in freshwater fishes. *Annu. Rev. Ecol. Syst.* **45**, 621–651 (2014). doi: [10.1146/annurev-ecolsys-120213-091818](https://doi.org/10.1146/annurev-ecolsys-120213-091818)
- L. Valente *et al.*, A simple dynamic model explains the diversity of island birds worldwide. *Nature* **579**, 92–96 (2020). doi: [10.1038/s41586-020-2022-5](https://doi.org/10.1038/s41586-020-2022-5); pmid: [32076267](https://pubmed.ncbi.nlm.nih.gov/32076267/)
- S. Gavrillets, J. B. Losos, Adaptive radiation: Contrasting theory with data. *Science* **323**, 732–737 (2009). doi: [10.1126/science.1157966](https://doi.org/10.1126/science.1157966); pmid: [19197052](https://pubmed.ncbi.nlm.nih.gov/19197052/)
- C. H. Martin, E. J. Richards, The paradox behind the pattern of rapid adaptive radiation: How can the speciation process sustain itself through an early burst? *Annu. Rev. Ecol. Syst.* **50**, 569–593 (2019). doi: [10.1146/annurev-ecolsys-110617-062443](https://doi.org/10.1146/annurev-ecolsys-110617-062443); pmid: [36237480](https://pubmed.ncbi.nlm.nih.gov/36237480/)
- S. J. Arnold, *Evolutionary Quantitative Genetics* (Oxford Univ. Press, 2023).
- S. Gavrillets, A. Vose, Dynamic patterns of adaptive radiation. *Proc. Natl. Acad. Sci. U.S.A.* **102**, 18040–18045 (2005). doi: [10.1073/pnas.0506330102](https://doi.org/10.1073/pnas.0506330102); pmid: [16330783](https://pubmed.ncbi.nlm.nih.gov/16330783/)
- O. Seehausen *et al.*, Genomics and the origin of species. *Nat. Rev. Genet.* **15**, 176–192 (2014). doi: [10.1038/nrg3644](https://doi.org/10.1038/nrg3644); pmid: [24535286](https://pubmed.ncbi.nlm.nih.gov/24535286/)
- D. Agashe, M. Sane, S. Singhal, Revisiting the role of genetic variation in adaptation. *Am. Nat.* **726012** (2023). doi: [10.1086/726012](https://doi.org/10.1086/726012)
- H. A. Orr, J. A. Coyne, The genetics of adaptation: A reassessment. *Am. Nat.* **140**, 725–742 (1992). doi: [10.1086/285437](https://doi.org/10.1086/285437); pmid: [19426041](https://pubmed.ncbi.nlm.nih.gov/19426041/)
- P. R. Grant, *Ecology and Evolution of Darwin's Finches* (Princeton Science Library Edition) (Princeton Univ. Press, 1986).
- S. Lamichhaney *et al.*, Evolution of Darwin's finches and their beaks revealed by genome sequencing. *Nature* **518**, 371–375 (2015). doi: [10.1038/nature14181](https://doi.org/10.1038/nature14181); pmid: [25686609](https://pubmed.ncbi.nlm.nih.gov/25686609/)
- S. Lamichhaney *et al.*, A beak size locus in Darwin's finches facilitated character displacement during a drought. *Science* **352**, 470–474 (2016). doi: [10.1126/science.aad8786](https://doi.org/10.1126/science.aad8786); pmid: [27102486](https://pubmed.ncbi.nlm.nih.gov/27102486/)
- J. A. Chaves *et al.*, Genomic variation at the tips of the adaptive radiation of Darwin's finches. *Mol. Ecol.* **25**, 5282–5295 (2016). doi: [10.1111/mec.13743](https://doi.org/10.1111/mec.13743); pmid: [27363308](https://pubmed.ncbi.nlm.nih.gov/27363308/)
- L. P. Lawson, K. Petren, The adaptive genomic landscape of beak morphology in Darwin's finches. *Mol. Ecol.* **26**, 4978–4989 (2017). doi: [10.1111/mec.14166](https://doi.org/10.1111/mec.14166); pmid: [28475225](https://pubmed.ncbi.nlm.nih.gov/28475225/)
- P. T. Boag, P. R. Grant, The classical case of character release: Darwin's finches (*Geospiza*) on Isla Daphne Major, Galápagos. *Biol. J. Linn. Soc. Lond.* **22**, 243–287 (1984). doi: [10.1111/j.1095-8312.1984.tb01679.x](https://doi.org/10.1111/j.1095-8312.1984.tb01679.x)
- P. T. Boag, P. R. Grant, Intense natural selection in a population of Darwin's finches (*geospizinae*) in the Galápagos. *Science* **214**, 82–85 (1981). doi: [10.1126/science.214.4516.82](https://doi.org/10.1126/science.214.4516.82); pmid: [17802577](https://pubmed.ncbi.nlm.nih.gov/17802577/)

22. P. R. Grant, B. R. Grant, Non-random fitness variation in two populations of Darwin's finches. *Proc. Biol. Sci.* **267**, 131–138 (2000). doi: [10.1098/rspb.2000.0977](https://doi.org/10.1098/rspb.2000.0977); pmid: 10687817
23. C. J. Rubin et al., Rapid adaptive radiation of Darwin's finches depends on ancestral genetic modules. *Sci. Adv.* **8**, eabm5982 (2022). doi: [10.1126/sciadv.abm5982](https://doi.org/10.1126/sciadv.abm5982); pmid: 35857449
24. K. Bombles, C. L. Peichel, Genetics of adaptation. *Proc. Natl. Acad. Sci. U.S.A.* **119**, e2122152119 (2022). doi: [10.1073/pnas.2122152119](https://doi.org/10.1073/pnas.2122152119); pmid: 35858399
25. R. D. H. Barrett, H. E. Hoekstra, Molecular spandrels: Tests of adaptation at the genetic level. *Nat. Rev. Genet.* **12**, 767–780 (2011). doi: [10.1038/nrg3015](https://doi.org/10.1038/nrg3015); pmid: 22005986
26. J. R. Stinchcombe, H. E. Hoekstra, Combining population genomics and quantitative genetics: Finding the genes underlying ecologically important traits. *Heredity* **100**, 158–170 (2008). doi: [10.1038/sj.hdy.6800937](https://doi.org/10.1038/sj.hdy.6800937); pmid: 17314923
27. S. Rubinacci, D. M. Ribeiro, R. J. Hofmeister, O. Delaneau, Efficient phasing and imputation of low-coverage sequencing data using large reference panels. *Nat. Genet.* **53**, 120–126 (2021). doi: [10.1038/s41588-020-00756-0](https://doi.org/10.1038/s41588-020-00756-0); pmid: 33414550
28. Materials and methods are available as supplementary materials.
29. S. Lamichaney et al., Female-biased gene flow between two species of Darwin's finches. *Nat. Ecol. Evol.* **6**, 979–986 (2020). doi: [10.1038/s41559-020-1183-9](https://doi.org/10.1038/s41559-020-1183-9); pmid: 32367030
30. P. R. Grant, B. R. Grant, J. A. Markert, L. F. Keller, K. Petren, Convergent evolution of Darwin's finches caused by introgressive hybridization and selection. *Evolution* **58**, 1588–1599 (2004). pmid: 15341160
31. P. R. Grant, B. R. Grant, Conspecific versus heterospecific gene exchange between populations of Darwin's finches. *Philos. Trans. R. Soc. Lond. B Biol. Sci.* **365**, 1065–1076 (2010). doi: [10.1098/rstb.2009.0283](https://doi.org/10.1098/rstb.2009.0283); pmid: 20194169
32. P. R. Grant, B. R. Grant, Triad hybridization via a conduit species. *Proc. Natl. Acad. Sci. U.S.A.* **117**, 7888–7896 (2020). doi: [10.1073/pnas.2000388117](https://doi.org/10.1073/pnas.2000388117); pmid: 32213581
33. P. R. Grant, R. B. Grant, *40 Years of Evolution: Darwin's Finches on Daphne Major Island* (Princeton Univ. Press, 2014).
34. P. R. Grant, B. R. Grant, K. Petren, A population founded by a single pair of individuals: Establishment, expansion, and evolution. *Genetica* **112**, 359–382 (2001). doi: [10.1023/A:1013363032724](https://doi.org/10.1023/A:1013363032724); pmid: 11838776
35. L. F. Keller, P. R. Grant, B. R. Grant, K. Petren, Heritability of morphological traits in Darwin's finches: Misidentified paternity and maternal effects. *Heredity* **87**, 325–336 (2001). doi: [10.1046/j.1365-2540.2001.00900.x](https://doi.org/10.1046/j.1365-2540.2001.00900.x); pmid: 11737279
36. J. Yang et al., Genetic variance estimation with imputed variants finds negligible missing heritability for human height and body mass index. *Nat. Genet.* **47**, 1114–1120 (2015). doi: [10.1038/ng.3390](https://doi.org/10.1038/ng.3390); pmid: 26323059
37. X. Zhou, M. Stephens, Efficient multivariate linear mixed model algorithms for genome-wide association studies. *Nat. Methods* **11**, 407–409 (2014). doi: [10.1038/nmeth.2848](https://doi.org/10.1038/nmeth.2848); pmid: 24531419
38. S. Wullschlegel, R. Loewith, M. N. Hall, TOR signaling in growth and metabolism. *Cell* **124**, 471–484 (2006). doi: [10.1016/j.cell.2006.01.016](https://doi.org/10.1016/j.cell.2006.01.016); pmid: 16469695
39. D. Melzer, L. C. Pilling, L. Ferrucci, The genetics of human aging. *Nat. Rev. Genet.* **21**, 88–101 (2020). doi: [10.1038/s41576-019-0183-6](https://doi.org/10.1038/s41576-019-0183-6); pmid: 31690828
40. R. Zoncu, A. Efeyan, D. M. Sabatini, mTOR: From growth signal integration to cancer, diabetes and ageing. *Nat. Rev. Mol. Cell Biol.* **12**, 21–35 (2011). doi: [10.1038/nrm3025](https://doi.org/10.1038/nrm3025); pmid: 21157483
41. K. Morrill et al., Ancestry-inclusive dog genomics challenges popular breed stereotypes. *Science* **376**, eabk0639 (2022). doi: [10.1126/science.abk0639](https://doi.org/10.1126/science.abk0639); pmid: 35482869
42. B. M. vonHoldt et al., Growth factor gene IGF1 is associated with bill size in the black-bellied seedcracker *Pyrenestes ostrinus*. *Nat. Commun.* **9**, 4855 (2018). doi: [10.1038/s41467-018-07374-9](https://doi.org/10.1038/s41467-018-07374-9); pmid: 30451848
43. S. E. McCaughy et al., Rapid molecular evolution across arthropods of the IIS/TOR network. *Proc. Natl. Acad. Sci. U.S.A.* **112**, 7055–7060 (2015). doi: [10.1073/pnas.1419659112](https://doi.org/10.1073/pnas.1419659112); pmid: 25991861
44. J. Pini et al., ALX1-related frontonasal dysplasia results from defective neural crest cell development and migration. *EMBO Mol. Med.* **14**, e16289 (2022). doi: [10.15252/emmm.202216289](https://doi.org/10.15252/emmm.202216289); pmid: 35795978
45. M. Bosse et al., Recent natural selection causes adaptive evolution of an avian polygenic trait. *Science* **358**, 365–368 (2017). doi: [10.1126/science.aal3298](https://doi.org/10.1126/science.aal3298); pmid: 29051380
46. LRR1Q1 leucine rich repeats and IQ motif containing 1 [Homo sapiens (human)]. NCBI; <https://www.ncbi.nlm.nih.gov/gene/84125>.
47. A. Abzhanov et al., The calmodulin pathway and evolution of elongated beak morphology in Darwin's finches. *Nature* **442**, 563–567 (2006). doi: [10.1038/nature04843](https://doi.org/10.1038/nature04843); pmid: 16885984
48. M. S. Almén et al., Adaptive radiation of Darwin's finches revisited using whole genome sequencing. *BioEssays* **38**, 14–20 (2016). doi: [10.1002/bies.201500079](https://doi.org/10.1002/bies.201500079); pmid: 26606649
49. L. Yengo et al., A saturated map of common genetic variants associated with human height. *Nature* **610**, 704–712 (2022). doi: [10.1038/s41586-022-05275-y](https://doi.org/10.1038/s41586-022-05275-y); pmid: 36224396
50. M. T. Webster et al., Linked genetic variants on chromosome 10 control ear morphology and body mass among dog breeds. *BMC Genomics* **16**, 474 (2015). doi: [10.1186/s12864-015-1702-2](https://doi.org/10.1186/s12864-015-1702-2); pmid: 26100605
51. M. Frischknecht et al., A non-synonymous *HMG2A* variant decreases height in shetland ponies and other small horses. *PLOS ONE* **10**, e0140749 (2015). doi: [10.1371/journal.pone.0140749](https://doi.org/10.1371/journal.pone.0140749); pmid: 26474182
52. C. J. Posbergh, H. J. Huson, All sheeps and sizes: A genetic investigation of mature body size across sheep breeds reveals a polygenic nature. *Anim. Genet.* **52**, 99–107 (2021). doi: [10.1111/age.13016](https://doi.org/10.1111/age.13016); pmid: 33089531
53. Z. Wu et al., Heterogeneity of a dwarf phenotype in Dutch traditional chicken breeds revealed by genomic analyses. *Evol. Appl.* **14**, 1095–1108 (2021). doi: [10.1111/evo.13183](https://doi.org/10.1111/evo.13183); pmid: 33897823
54. M. O. Lee et al., Hmga2 deficiency is associated with allometric growth retardation, infertility, and behavioral abnormalities in mice. *G3* **12**, jkab417 (2022). doi: [10.1093/g3journal/jkab417](https://doi.org/10.1093/g3journal/jkab417)
55. M. Carneiro et al., Dwarfism and altered craniofacial development in rabbits is caused by a 12.1 kb deletion at the *HMG2A* locus. *Genetics* **205**, 955–965 (2017). doi: [10.1534/genetics.116.196667](https://doi.org/10.1534/genetics.116.196667); pmid: 27986804
56. J. Chung et al., High mobility group A2 (HMG2A) deficiency in pigs leads to dwarfism, abnormal fetal resource allocation, and cryptorchidism. *Proc. Natl. Acad. Sci. U.S.A.* **115**, 5420–5425 (2018). doi: [10.1073/pnas.1721630115](https://doi.org/10.1073/pnas.1721630115); pmid: 29375702
57. J. Hellemans et al., Loss-of-function mutations in *LEM3D3* result in osteopikilosis, Buschke-Ollendorff syndrome and melorheostosis. *Nat. Genet.* **36**, 1213–1218 (2004). doi: [10.1038/ng1453](https://doi.org/10.1038/ng1453); pmid: 15489854
58. O. Campàs, R. Mallarino, A. Herrel, A. Abzhanov, M. P. Brenner, Scaling and shear transformations capture beak shape variation in Darwin's finches. *Proc. Natl. Acad. Sci. U.S.A.* **107**, 3356–3360 (2010). doi: [10.1073/pnas.0911575107](https://doi.org/10.1073/pnas.0911575107); pmid: 20160106
59. P. R. Grant, B. R. Grant, Unpredictable evolution in a 30-year study of Darwin's finches. *Science* **296**, 707–711 (2002). doi: [10.1126/science.1070315](https://doi.org/10.1126/science.1070315); pmid: 11976447
60. P. R. Grant, B. R. Grant, Evolution of character displacement in Darwin's finches. *Science* **313**, 224–226 (2006). doi: [10.1126/science.1128374](https://doi.org/10.1126/science.1128374); pmid: 16840700
61. H. A. Orr, The population genetics of adaptation: The distribution of factors fixed during adaptive evolution. *Evolution* **52**, 935–949 (1998). doi: [10.2307/2411226](https://doi.org/10.2307/2411226); pmid: 28565213
62. J. K. Pritchard, A. Di Rienzo, Adaptation - not by sweeps alone. *Nat. Rev. Genet.* **11**, 665–667 (2010). doi: [10.1038/nrg2880](https://doi.org/10.1038/nrg2880); pmid: 20838407
63. D. L. Stern, V. Orgogozo, The loci of evolution: How predictable is genetic evolution? *Evolution* **62**, 2155–2177 (2008). doi: [10.1111/j.1558-5646.2008.00450.x](https://doi.org/10.1111/j.1558-5646.2008.00450.x); pmid: 18616572
64. J. Zeng et al., Signatures of negative selection in the genetic architecture of human complex traits. *Nat. Genet.* **50**, 746–753 (2018). doi: [10.1038/s41588-018-0101-4](https://doi.org/10.1038/s41588-018-0101-4); pmid: 29662166
65. J. S. Sanjak, J. Sidorenko, M. R. Robinson, K. R. Thornton, P. M. Visscher, Evidence of directional and stabilizing selection in contemporary humans. *Proc. Natl. Acad. Sci. U.S.A.* **115**, 151–156 (2018). doi: [10.1073/pnas.1707227114](https://doi.org/10.1073/pnas.1707227114); pmid: 29255044
66. J. Gutiérrez-Valencia, P. W. Hughes, E. L. Berdan, T. Slotte, The genomic architecture and evolutionary fates of supergenes. *Genome Biol. Evol.* **13**, evab057 (2021). doi: [10.1093/gbe/evab057](https://doi.org/10.1093/gbe/evab057); pmid: 33739390
67. M. Kirkpatrick, N. Barton, Chromosome inversions, local adaptation and speciation. *Genetics* **173**, 419–434 (2006). doi: [10.1534/genetics.105.047985](https://doi.org/10.1534/genetics.105.047985); pmid: 16204214
68. S. Yeaman, M. C. Whitlock, The genetic architecture of adaptation under migration-selection balance. *Evolution* **65**, 1897–1911 (2011). doi: [10.1111/j.1558-5646.2011.01269.x](https://doi.org/10.1111/j.1558-5646.2011.01269.x); pmid: 21729046
69. N. B. Edelman et al., Genomic architecture and introgression shape a butterfly radiation. *Science* **366**, 594–599 (2019). doi: [10.1126/science.aaw2090](https://doi.org/10.1126/science.aaw2090); pmid: 31672890
70. O. Savolainen, M. Lascoux, J. Merilä, Ecological genomics of local adaptation. *Nat. Rev. Genet.* **14**, 807–820 (2013). doi: [10.1038/nrg3522](https://doi.org/10.1038/nrg3522); pmid: 24136507
71. S. L. Lundregan et al., Inferences of genetic architecture of bill morphology in house sparrow using a high-density SNP array point to a polygenic basis. *Mol. Ecol.* **27**, 3498–3514 (2018). doi: [10.1111/mec.14811](https://doi.org/10.1111/mec.14811); pmid: 30040161
72. P. R. Grant, B. R. Grant, Mating patterns of Darwin's Finch hybrids determined by song and morphology. *Biol. J. Linn. Soc. Lond.* **60**, 317–343 (1997). doi: [10.1111/1095-8312.1997.tb0499.x](https://doi.org/10.1111/1095-8312.1997.tb0499.x)
73. E. D. Embody et al., A multispecies BCO2 beak color polymorphism in the Darwin's finch radiation. *Curr. Biol.* **31**, 5597–5604.e7 (2021). doi: [10.1016/j.cub.2021.09.085](https://doi.org/10.1016/j.cub.2021.09.085); pmid: 34687609
74. S. Picelli et al., Trn5 transposase and tagmentation procedures for massively scaled sequencing projects. *Genome Res.* **24**, 2033–2040 (2014). doi: [10.1101/gr.177881.114](https://doi.org/10.1101/gr.177881.114); pmid: 25079858
75. C. G. Sprehn, E. Embody, Y. Zan, L. Andersson, Trn5 based tagmentation library prep protocol, high throughput v1 (2021). doi: [10.175504/protocols.io.bv5gn83w](https://doi.org/10.175504/protocols.io.bv5gn83w)
76. M. Martin et al., WhatsHap: fast and accurate read-based phasing. *bioRxiv* (2016), p. 085050.
77. O. Delaneau, J.-F. Zagury, M. R. Robinson, J. L. Marchini, E. T. Dermizakis, Accurate, scalable and integrative haplotype estimation. *Nat. Commun.* **10**, 5436 (2019). doi: [10.1038/s41467-019-13225-y](https://doi.org/10.1038/s41467-019-13225-y); pmid: 31780650
78. P. Rastias, Lep-MAP3: Robust linkage mapping even for low-coverage whole genome sequencing data. *Bioinformatics* **33**, 3726–3732 (2017). doi: [10.1093/bioinformatics/btx494](https://doi.org/10.1093/bioinformatics/btx494); pmid: 29036272
79. D. H. Alexander, J. Novembre, K. Lange, Fast model-based estimation of ancestry in unrelated individuals. *Genome Res.* **19**, 1655–1664 (2009). doi: [10.1101/gr.094052.109](https://doi.org/10.1101/gr.094052.109); pmid: 19648217
80. J. Yang, S. H. Lee, M. E. Goddard, P. M. Visscher, GCTA: A tool for genome-wide complex trait analysis. *Am. J. Hum. Genet.* **88**, 76–82 (2011). doi: [10.1016/j.ajhg.2010.11.011](https://doi.org/10.1016/j.ajhg.2010.11.011); pmid: 21167468
81. P. Cingolani et al., A program for annotating and predicting the effects of single nucleotide polymorphisms, SnpEff: SNPs in the genome of *Drosophila melanogaster* strain w1118; iso-2; iso-3. *Fly* **6**, 80–92 (2012). doi: [10.4161/fly.19695](https://doi.org/10.4161/fly.19695); pmid: 22728672
82. E. Embody, Data associated with Embody et al., 2023, Zenodo (2023); <https://dx.doi.org/10.5281/zenodo.8044096>.

## ACKNOWLEDGMENTS

We thank J. Sidorenko for assistance in processing UK Biobank data, R. Corbett-DeGis for insightful discussion, and A. Cocco and J. Pettersson for assistance in the lab. The National Genomics Infrastructure (NGI)/Uppsala Genome Center provided service in massive parallel sequencing, and the computational infrastructure was provided by the Swedish National Infrastructure for Computing at UPPMAX, partially funded by the Swedish Research Council grant agreement no. 2018-05973. This study used genotype and phenotype data from the UK Biobank resource under approved project 12505. The National Science Foundation funded the collection of material under permits from the Galápagos National Parks Service and the Charles Darwin Research Station, and in accordance with protocols of Princeton University's Animal Welfare Committee. **Funding:** This project was financially supported by Vetenskapsrådet (2017-02907) and the Knut and Alice Wallenberg Foundation (KAW 2016.0361).

**Author contributions:** Conceptualization: L.A., P.R.G., B.R.G., and E.D.E.; Data curation: C.G.S. and E.D.E.; Methodology: E.D.E. and L.A.; Formal analysis: E.D.E., A.S.P., C.J.R., and P.M.V.; Investigation: C.G.S., E.D.E., P.R.G., and B.R.G.; Visualization: E.D.E. and A.S.P.; Funding acquisition: L.A., P.R.G., and B.R.G.; Resources: P.R.G. and B.R.G. Supervision: L.A. Writing – original draft: E.D.E. Writing – review and editing: all authors. **Competing interests:** The authors declare that they have no competing interests. **Data and materials availability:** All custom code is available at Zenodo (82). Sequence data in this study have been deposited in the Sequence Read Archive under BioProject PRJNA897926. **License information:** Copyright © 2023 the authors, some rights reserved; exclusive licensee American Association for the Advancement of Science. No claim to original US government works. <https://www.science.org/about/science-licenses-journal-article-reuse>

## SUPPLEMENTARY MATERIALS

[science.org/doi/10.1126/science.adf6218](https://doi.org/10.1126/science.adf6218)

Materials and Methods

Supplementary Notes S1 to S5

Figs. S1 to S26

Table S1 to S6

References (83–113)

Submitted 7 November 2022; accepted 22 August 2023

10.1126/science.adf6218



## Community-wide genome sequencing reveals 30 years of Darwin's finch evolution

Erik D. Enbody, Ashley T. Sendell-Price, C. Grace Sprehn, Carl-Johan Rubin, Peter M. Visscher, B. Rosemary Grant, Peter R. Grant, and Leif Andersson

*Science* **381** (6665), eadf6218. DOI: 10.1126/science.adf6218

### Editor's summary

The ability of an organism to respond to shifting selective pressures depends on the genetic architectures of the traits underlying adaptations. Examining four species of Darwin's finches from the Galápagos Islands, Enbody *et al.* identified six loci with large effects on beak size that explain 59% of the total heritability in one of these species. The authors also connect the incidence of droughts, which result in changes in food availability, to shifts in the allele frequency of these loci, some of which are caused by hybridization between species. This study takes advantage of 30 years of study of a classic system to elucidate the role of genetic architecture and introgression in adaptation. — Corinne Simonti

### View the article online

<https://www.science.org/doi/10.1126/science.adf6218>

### Permissions

<https://www.science.org/help/reprints-and-permissions>

Use of this article is subject to the [Terms of service](#)

---

*Science* (ISSN 1095-9203) is published by the American Association for the Advancement of Science. 1200 New York Avenue NW, Washington, DC 20005. The title *Science* is a registered trademark of AAAS.

Copyright © 2023 The Authors, some rights reserved; exclusive licensee American Association for the Advancement of Science. No claim to original U.S. Government Works